OPEN ACCESS
CellPress

Cell Reports
Article

Multilineage Potential and Self-Renewal Define an Epithelial Progenitor Cell Population in the Adult Thymus

Kahlia Wong,[1,4] Natalie L. Lister,[1,4] Marco Barsanti,[1] Joanna M.C. Lim,[1] Maree V. Hammett,[1] Danika M. Khong,[1,2] Christopher Siatskas,[1] Daniel H.D. Gray,[3] Richard L. Boyd,[1] and Ann P. Chidgey[1,*]

[1]Stem Cells and Immune Regeneration Laboratory, Department of Anatomy and Developmental Biology, Monash University, Wellington Road, Clayton, VIC 3800, Australia

[2]Harvard Stem Cell and Regenerative Biology, Harvard Stem Cell Institute, Boston, MA 02138, USA

[3]Molecular Genetics of Cancer Division and Immunology Division, The Walter and Eliza Hall Institute, Parkville, VIC 3052, Australia

[4]Co-first author

*Correspondence: ann.chidgey@monash.edu

http://dx.doi.org/10.1016/j.celrep.2014.07.029

SUMMARY

Thymic epithelial cells (TECs) are critical for T cell development and self-tolerance but are gradually lost with age. The existence of thymic epithelial progenitors (TEPCs) in the postnatal thymus has been inferred, but their identity has remained enigmatic. Here, we assessed the entire adult TEC compartment in order to reveal progenitor capacity is retained exclusively within a subset of immature thymic epithelium displaying several hallmark features of stem/progenitor function. These adult TEPCs generate mature cortical and medullary lineages in a stepwise fashion, including Aire+ TEC, within fetal thymus reaggregate grafts. Although relatively quiescent in vivo, adult TEPCs demonstrate significant in vitro colony formation and self-renewal. Importantly, 3D-cultured TEPCs retain their capacity to differentiate into cortical and medullary TEC lineages when returned to an in vivo thymic microenvironment. No other postnatal TEC subset exhibits this combination of properties. The characterization of adult TEPC will enable progress in understanding TEC biology in aging and regeneration.

INTRODUCTION

The thymus is required to produce functional T cells vital for cell-mediated immune responses against invading pathogens and malignant cells (Anderson and Takahama, 2012). The postnatal thymus is composed of outer cortical and inner medulla regions through which thymocytes (T cell precursors) migrate in a directed fashion as they undergo distinct stages of differentiation. Cortical thymic epithelial cells (cTECs) and subcapsular epithelia provide soluble and cell-bound signals for initial attraction of circulating hematopoietic precursors, lineage commitment, and positive selection of thymocytes expressing functional T cell receptors (Anderson and Takahama, 2012). Presentation of tissue-restricted antigens by medullary TEC (mTECs) and dendritic cells mediate negative selection of autoreactive thymocytes (Metzger and Anderson, 2011). Together, the availability of functional cortical and medullary thymic epithelial niches critically limits central T cell output (Jenkinson et al., 2007; Cheng et al., 2010).

Thymic function declines naturally with age and is characterized by TEC loss and a decline in naive T cell output. Moreover, cytoreductive treatments associated with cancer therapy and hematopoietic stem cell transplantation cause collateral damage to thymic structure and function (Haynes et al., 2000). Regenerating TEC is an important goal to overcoming the resulting, often prolonged, immune deficiencies (Chidgey et al., 2007). Several lines of evidence strongly support a model in which a reservoir of stem/progenitor TECs within the adult murine thymus retains substantial capacity to regenerate thymic tissue following damage (Chidgey et al., 2008; Rode and Boehm, 2012). Moreover, the rapid turnover of mature mTECs expressing the autoimmune regulator (Aire) suggests continual homeostatic replacement (Gray et al., 2006; Metzger et al., 2013). Despite evidence of their existence (Bleul et al., 2006), difficulties in the identification, prospective isolation, and functional validation of viable adult thymic epithelial progenitor (TEPC) candidates have hindered progress in this field.

Fetal TEPCs have been identified by the cell-surface expression of Plet-1 using the monoclonal antibody MTS24 (Bennett et al., 2002; Gill et al., 2002; Depreter et al., 2008) and by the cortical marker DEC205 (Baik et al., 2013), whereas recent lineage-tracing studies have shown the majority of postnatal TEC lineages were originally derived from precursors expressing the cTEC-specific β5t proteasome subunit (Ohigashi et al., 2013). Bipotent TEPCs present in fetal (Rossi et al., 2006) and postnatal thymic tissue (Bleul et al., 2006) were shown to generate both mTEC and cTEC lineages; however, their phenotype and location were not defined. In addition, several lines of evidence also support the existence of downstream, lineage-restricted progenitors within medullary and cortical compartments (Rodewald et al., 2001; Bleul et al., 2006; Hamazaki et al., 2007; Shakib et al., 2009).

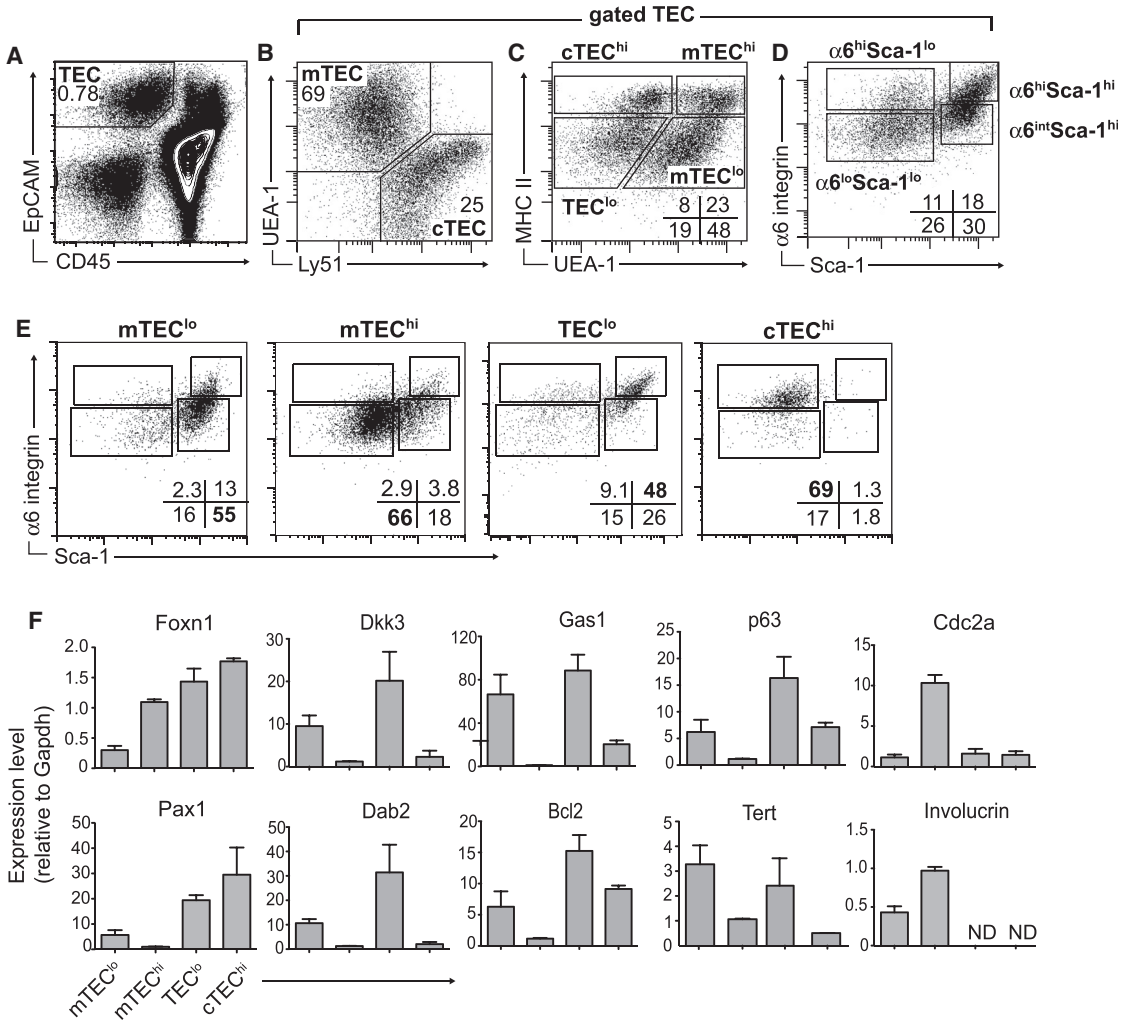

Figure 1. Phenotypic Analysis of Adult TEC Subsets

(A) Adult thymic digests show gating of TECs.

(B) UEA-1 and anti-Ly51 staining discriminates mTEC (UEA-1$^+$ Ly51$^-$) and cTEC (UEA-1$^-$ Ly51$^+$) subpopulations.

(C) UEA-1 and anti-MHCII delineate four TEC subsets: mTEC^{hi}, mTEC^{lo}, cTEC^{hi}, and TEC^{lo}.

(D) Expression of α6 integrin and Sca-1 in TECs, with regions demarcating four populations: α6^{hi}Sca-1^{lo}, α6^{lo}Sca-1^{lo}, α6^{hi}Sca-1^{hi}, and α6^{int}Sca-1^{hi}.

(E) Expression of α6 integrin and Sca-1 on gated TEC subsets.

(F) Purified adult TEC subsets were analyzed for gene transcripts with mean expression level (+SEM) plotted relative to mTEC^{hi}. Data representative of ΔCt triplicates pooled from three independent experiments. ND, not detected.

See also Figure S1.

Despite extensive studies, how the TEC precursor-product relationships observed in the embryo or early neonate relate to the adult thymus is yet to be elucidated. It is also unclear whether progenitors identified by surface markers in the fetal thymus correspond functionally to their adult counterpart, mainly due to a paucity of culture conditions that support the functional assessment of adult TEC. To resolve these issues, discrete adult TEC subsets were purified and assessed for progenitor function using both in vivo fetal thymus reaggregate grafts (Jenkinson et al., 1992) and a 3D in vitro culture system developed herein. Our data reveal that substantial self-renewal capacity and multilineage differentiation potential within the postnatal TEC pool is contained exclusively within a subset of immature TEC expressing low levels of major histocompatibility complex II (MHCII) and high levels of stem-cell-associated surface proteins, α6-integrin and stem cell antigen-1 (Sca-1).

RESULTS

Identification of Candidate Adult Thymic Epithelial Progenitor Subsets

In the adult thymus, considerable heterogeneity exists within the epithelial compartment (Seach et al., 2012). Adult TECs express the epithelial cell adhesion molecule (EpCAM) and are negative for the hematopoietic-lineage marker CD45 (Figure 1A). Using multiparameter flow cytometry (fluorescence-activated

cell sorting [FACS]) analysis, TECs were broadly defined into Ulex europaeus agglutinin-1 (UEA-1)$^{+}$ Ly51^{-} mTECs and UEA-1^{-} Ly51$^{lo/hi}$ cTECs (Figure 1B; Seach et al., 2012). Adult TECs were then further divided into discrete subsets based on high or low levels of MHCII expression: TEC^{lo} (MHCII^{lo}UEA-1^{-}Ly51^{lo}), cTEC^{hi} (MHCII^{hi}UEA-1^{-}Ly51^{hi}), mTEC^{lo} (MHCII^{lo}UEA-1^{+}Ly51^{-}), and mTEC^{hi} (MHCII^{hi}UEA-1^{+}Ly51^{-}), subpopulations based on MHCII versus UEA-1 (Figure 1C) or MHCII versus Ly51 expression levels (Figure S1A). Analysis of markers defining fetal TEPC such as DEC205 and intracellular β5t antigens, revealed that, in the adult, DEC205 was expressed across both TEC^{lo} and cTEC^{hi} subsets (Figure S1B) and β5t expression was confined predominantly within the cTEC^{hi} subset (Figure S1C).

These adult TEC subsets were further interrogated for expression of known epithelial stem cell surface markers and transcripts. High cell-surface expression of α6-integrin (α6; CD49f) and/or Sca-1 identifies cells with stem or progenitor potential in numerous epithelial tissues, including the epidermis (Terunuma et al., 2007), cornea (Hayashi et al., 2008), breast (Welm et al., 2002), and lung (McQualter et al., 2010). FACS analysis showed that at embryonic day 15 (E15) fetal TECs were largely Sca-1 negative and uniformly expressed low levels of α6 integrin (Figure S1D). Upregulation of Sca-1 commenced around E18, and by neonatal day 3, a prominent α6^{hi}Sca-1^{hi} TEC subset was detected that persisted into adulthood, with differential distribution of α6/Sca-1 among the four major TEC subsets (Figures 1D and 1E). The TEC^{lo} cells were predominantly α6^{hi}Sca-1^{hi} in phenotype (48% ± 6.4%); whereas mTEC^{lo} were mainly α6^{int}Sca-1^{hi} (52% ± 5.9%). Most cTEC^{hi} cells also expressed high surface levels of α6 but were distinguished from TEC^{lo} by low-level Sca-1 staining (α6^{hi}Sca-1^{lo}; 67.1% ± 3.6%). In contrast, mTEC^{hi} expressed low α6 and Sca-1 levels (α6^{lo}Sca-1^{lo}; 68% ± 3.5%), compatible with reports that mTEC^{hi} represent a mature mTEC population (Gray et al., 2007; Yano et al., 2008).

Quantitative RT-PCR revealed that TEC^{lo} and (to a lesser extent) mTEC^{lo} subsets were enriched for gene transcripts implicated in epithelial stem/progenitor cell regulation. These included Wnt-inhibitors *Dkk3* and *Dab2*, which control proliferation and differentiation of stem cells (SCs) into lineage-restricted cells (Morris et al., 2004); cell-cycle suppressor gene, *Gas1* (Tumbar et al., 2004); antiapoptotic gene, *Bcl2* (Adams and Cory, 1998); epithelial-progenitor-associated gene, *p63* (Senoo et al., 2007); and telomerase reverse transcriptase, *Tert*, suggestive of self-renewal properties (Hiyama and Hiyama, 2007; Figure 1E). The transcriptional regulator *Pax1* is expressed during early fetal thymus and parathyroid gland development and is progressively restricted to cTEC in postnatal tissue (Wallin et al., 1996). In accordance, *Pax1* mRNA was strongly expressed in both TEC^{lo} and cTEC^{hi} subsets and reduced in mTEC subsets (Figure 1E). Expression of *Foxn1*, essential for early TEC differentiation, was detected in all adult TEC subsets (Figure 1E). Consistent with the notion that the mTEC^{hi} subset contains both transit amplifying (TA) and postmitotic, terminally differentiated cells (Gray et al., 2007), this population contained the highest expression levels of cyclin-dependent kinase 2a (*Cdc2a*) (characteristic of TA cells), *involucrin* (a putative marker of terminally differentiated epithelium in skin; Fuchs, 1990), and thymus (Yano et al., 2008; Figure 1E). Collectively, these results reveal differential expression of stem-cell-associated genes and cell-surface molecules within the adult TEC compartment and suggest that progenitor potential may reside preferentially within TEC^{lo}/mTEC^{lo} subsets.

Quiescent Label-Retaining Cells Reside within the TEC^{lo} Subset

Label-retention studies using nucleoside analogs have been used to exploit nonsenescent, quiescent properties of tissue-specific stem/progenitor cells and facilitate their phenotypic identification and in vivo location (Blanpain and Fuchs, 2006). To identify label-retaining cells (LRC) within postnatal TEC, young adult mice were exposed to 5-bromo-2′-deoxyuridine (BrdU) for a 12-day pulse period, after which BrdU was withdrawn and TEC subsets assessed for label retention over a 6-month chase. Importantly, no changes in thymic cellularity were observed at the end of the 12-day pulse period, indicating an absence of BrdU-related thymic toxicity (data not shown).

FACS analysis revealed that the proportion of BrdU^{+} adult TECs accumulated steadily over the pulse period, reaching an average of 27.8% ± 1.1% BrdU^{+} TECs by the end (Figure 2A). BrdU^{+} TECs were rapidly lost following withdrawal, decreasing to approximately 5% ± 0.3% of total TEC at 1 month, then declining further to a mean of 1.2% ± 0.2% of total TECs at 6 months chase (Figures 2A and 2B). Importantly, at day 12 of pulse, BrdU^{+} TECs were distributed within both UEA-1^{+} Ly51^{-} mTEC (69.2% ± 4.5%) and, to a lesser extent, UEA-1^{-} Ly51^{+} cTEC (24.1% ± 4.5%) compartments (Figure 2C), with incorporation evident throughout all TEC subsets (Figures 2D and 2E). mTEC^{hi} incorporated the most label (34.4% ± 1%) during the pulse period, followed by mTEC^{lo} and cTEC^{hi} subsets (21% ± 1.1% and 23.8% ± 2.5%, respectively; Figures 2D and 2F). TEC^{lo} had the lowest proportion of BrdU^{+} TEC (10.8% ± 0.9%), suggesting a relatively low turnover of these cells.

After a 6-month chase period, most BrdU^{+} cells were lost; however, a clear LRC population remained, of which 71.8% ± 3% were TEC^{lo} in phenotype (Figure 2D). Most of these LRCs also expressed high levels of α6 and Sca-1 surface protein (54.4% ± 4.3%; Figure 2E), indicative of a stem/progenitor subpopulation. The proportion of BrdU^{+} cells within the cTEC^{hi}, mTEC^{lo}, or mTEC^{hi} subsets gradually declined over the 6-month chase period. By contrast, the proportion of BrdU^{+} cells within the TEC^{lo} subset increased, indicating the retention of BrdU label by a specific subpopulation within this subset (Figures 2F and S2A).

Immunofluorescence analysis of 6-month BrdU-pulsed thymic lobes revealed the presence of rare, single BrdU^{+} TECs that costained with keratin and DAPI, indicative of label-retaining TECs (Figures S2B–S2E). Some BrdU^{+} TECs were found within separate cortical and medullary regions, defined by DEC205 (Figure S2B) and keratin 5 (K5) (Figure S2C) staining, respectively, but the majority of LRCs (~54%) were found at the cortico-medullary junction (Figures S2D and S2E).

Collectively, our data reveal that a subpopulation of TEC^{lo} retained BrdU label over a long-term period, reflective of a quiescent stem/progenitor subset. These putative TEPCs expressed high levels of α6/Sca-1 and preferentially resided at the cortico-medullary junction. To directly address adult TEPC

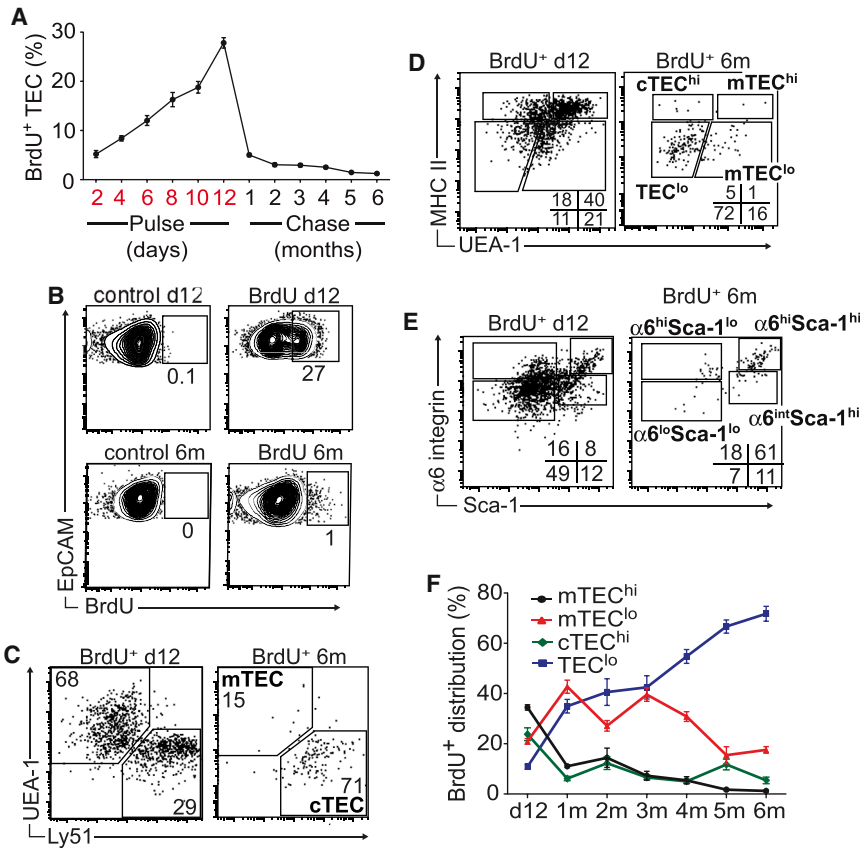

Figure 2. BrdU Label Retention within Adult Thymic Epithelium

(A) Graph shows mean proportion (±SEM) of BrdU$^+$ TECs (CD45$^-$ EpCAM$^+$) over a 12-day (d) pulse period and 6-month (m) chase.

(B) Plots show percentage BrdU$^+$ TECs from control mice or BrdU-treated mice at day 12 and 6 months.

(C–E) Distribution of BrdU$^+$ TECs within medullary (mTEC), cortical (cTEC), and TEC^{lo} subsets (C) and TEC subsets defined by UEA-1 and anti-MHCII (D) or anti-α6-integrin and anti-Sca-1 staining (E) at day 12 (left panel) or 6 months (right panel).

(F) Graph shows the mean proportion (±SEM) of BrdU$^+$ TEC distribution within TEC subsets at day 12 pulse and 1–6 months chase period. Data representative of two experiments, with n = 4 per time point.

See also Figure S2.

properties of self-renewal and differentiation, we used in vivo and in vitro systems to assess their stem/progenitor function.

Adult TEPCs Generate Medullary Lineage In Vivo

The differentiation of precursor epithelium into mature TEC subsets represented in adult thymus tissue requires reciprocal interactions with lymphoid cells (Anderson and Jenkinson, 2001). Therefore, to assess the differentiation potential of individual adult TEC subsets, we utilized reaggregate thymic organ cultures (RTOCs), a technique enabling the aggregation of defined fetal thymic stromal and hematopoietic components for the assessment of thymus function (Jenkinson et al., 1992). Adult TEC subsets (TEC^{lo}, cTEC^{hi}, mTEC^{lo}, and mTEC^{hi}) were purified from ubiquitous GFP transgenic mice and reaggregated with whole fetal (E14.5) thymus cells and engrafted under the kidney capsule to allow thymus formation (Figure 3A). Resulting ectopic fetal thymic grafts generated defined cortical and medullary regions, supported normal thymopoiesis, and incorporated GFP$^+$ adult TEPCs into the thymic microenvironment (Figure 3B).

At 6 weeks, reaggregate grafts were analyzed by FACS for the presence of GFP$^+$ EpCAM$^+$ adult-derived TEC and lineage-restricted markers. A consistent population of GFP$^+$ TECs was recovered from all purified adult TEC^{lo} grafts (9/9 grafts), representing on average 1.78% ± 0.3% of total TECs (Figures 3C and 3D). A minimal proportion of GFP$^+$ TECs (0.23% ± 0.1%) were recovered from half of the cTEC^{hi} grafts (3/6), and almost no GFP$^+$ TECs were recovered from grafts containing adult mTEC^{lo} (1/10) and mTEC^{hi} (0/7) subsets or control grafts containing fetal thymus alone (0/6; Figure 3D). These data indicate that, consistent with BrdU label-retaining studies, adult TEPCs reside preferentially within the TEC^{lo} subset. Phenotypic staining revealed both GFP$^+$UEA-1$^+$ mTEC and GFP$^+$Ly51$^+$ cTEC subsets were generated from grafts containing adult TEPCs (Figure 3E), including all four mTEC^{hi}, mTEC^{lo}, cTEC^{hi}, and TEC^{lo} subpopulations (Figure 3E). GFP$^+$ TEC subsets were observed at similar proportions in reaggregate grafts to those represented in an endogenous adult thymus (Figure 3F). Whereas LRCs were preferentially enriched within the α6^{hi}Sca-1^{hi} phenotype, further partitioning of TEC^{lo} into α6^{hi}Sca-1^{hi} and α6^{int}Sca-1^{hi} subsets and assessment within fetal thymus reaggregate grafts did not enrich for TEPC potential. Importantly, the α6^{lo}Sca-1^{lo} TEC^{lo} subset did not persist within thymic grafts (data not shown).

The absence of GFP$^+$ TECs recovered from adult mTEC^{lo} grafts was notable given previous findings that this subset contains precursors of the Aire$^+$ mTEC^{hi} lineage and was retained in short-term RTOCs (Gray et al., 2007). Indeed, analysis of reaggregate grafts seeded with mTEC^{lo} (supplemented with single positive thymocytes) at earlier time points revealed the presence of an mTEC^{hi} subset at 1 week postengraftment; however, no GFP$^+$ TECs were recovered at subsequent time points (data not shown). Thus, despite some enrichment of stem-cell-associated genes and phenotypic markers associated with progenitor function, mTEC^{lo} precursors do not persist in reaggregate grafts, indicating they possess a limited ability to self-renew and are most likely maintained by upstream progenitors. In contrast, TEPCs within the adult TEC^{lo} subset could persist in reaggregate thymic grafts and generate multiple downstream lineages indicative of significant stem/progenitor function.

To investigate the route by which cTEC and mTEC subsets were generated from adult TEPCs, we analyzed GFP$^+$ TEC^{lo} fetal thymus reaggregate grafts at earlier time points (Figure 3G).

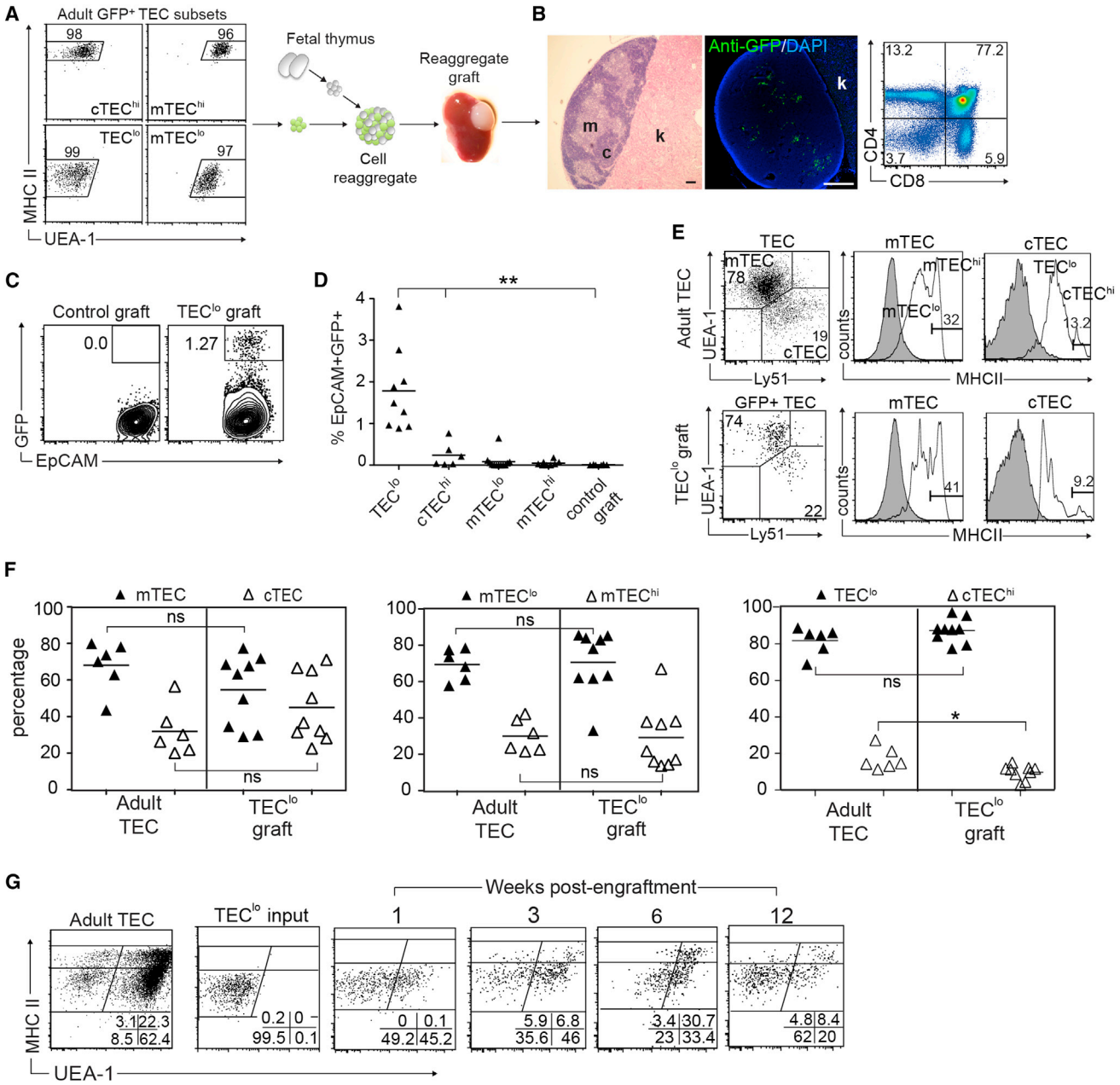

Figure 3. Differentiation of Adult Thymic Epithelial Progenitors In Vivo

(A) Purified GFP$^+$ adult TEC subsets were reaggregated with E14.5 whole fetal thymus cells and engrafted under the kidney capsule; plots are representative of 6–12 experiments.

(B) Data show 6-week TEPC reaggregate graft; hematoxylin and eosin staining showing cortical (c) and medullary (m) regions (scale bar represents 100 μm); IF image shows GFP$^+$ adult TEPCs revealed with anti-GFP (green; DAPI, blue; k, kidney; scale bar represents 500 μm); dot plot shows normal thymocyte development within graft.

(C) Recovery of GFP$^+$TECs from grafts containing E14.5 fetal thymus alone (control) or mixed with purified adult TEC^{lo}.

(D) Scatter plot shows the percentage of GFP$^+$ TECs recovered from individual control grafts or grafts containing purified adult TEC subsets as indicated; $^{**}p < 0.01$.

(E) UEA-1 and anti-Ly51 staining profiles show respective mTEC and cTEC subsets, whereas gated MHCII histograms indicate mTEC^{hi} mTEC^{lo} and cTEC^{hi} and TEC^{lo} subsets within normal adult TECs or GFP$^+$ TECs recovered from TEPC reaggregate grafts; plots are representative of individual grafts (n = 12) or adult thymic digests (n = 8) over five individual experiments.

(F) Scatter plots show the proportion of individual TEC subsets from adult wild-type (WT) control thymus or GFP$^+$ TECs recovered from TEC^{lo} grafts as gated in (E); horizontal line indicates mean; $^{*}p < 0.05$.

(legend continued on next page)

By 1 week, grafts contained a substantial proportion of adult GFP$^+$ TECs that had upregulated UEA-1 while maintaining low levels of MHCII, indicative of differentiation into an mTEC^{lo} phenotype (53.4% ± 2.4%; Figure 3G). A small subset of mTEC^{hi} had appeared by 3 weeks (7.6% ± 1.1%), which had expanded by 6 weeks (28.7% ± 5.5%). At 3 weeks, the emergence of rare UEA-1$^-$ MHCII^{hi} cells (6.3% ± 1.1%), representative of the cTEC^{hi} phenotype, was observed and retained within both 6-week (4.7% ± 1.4%) and 12-week (5.3% ± 0.8%) grafts (Figure 3G); these cells expressed Ly51, indicative of their cortical phenotype (Figure 3E; data not shown). Notably, a substantial TEC^{lo} subset was maintained throughout the graft time course, and at 12 weeks, all adult TEC subsets were still represented, indicating the persistence of a TEPC subpopulation capable of maintaining downstream TEC lineages within thymic grafts (Figures 3G and S3).

Analysis of 6-week adult TEC^{lo} reaggregate grafts by immunohistology revealed small, isolated pockets of GFP$^+$ cells distributed throughout the thymic microenvironment (Figure 4A). All GFP$^+$ cells colocalized with pan-keratin, confirming epithelial cell origin (Figure 4B). To determine whether these clusters were clonally derived from single TEPC or due to cell aggregation, in vitro reaggregates were formed by combining equal numbers of adult TEPCs isolated from transgenic mice ubiquitously expressing GFP or red fluorescent protein (RFP) for grafting. Four weeks later, >99% of islet clusters were found to consist entirely of GFP$^+$ or RFP$^+$ cells, indicating that islets most likely consisted of TECs generated from single adult progenitors as opposed to mixed progenitor aggregation (Figure 4C). Antibody costaining revealed the majority (15/21) of GFP$^+$ islets contained TECs that were DEC205$^+$ (cTEC marker) and K5$^+$ (mTEC/cortico-medullary junction marker); however, due to the relatively small size of islets, distinct medullary and cortical regions were not clearly defined (Figure 4D). In addition, some islets contained Aire$^+$ TEC (5/30) indicative of the mature mTEC lineage (Figure 4E); islets containing Aire$^+$ TECs were also found to contain DEC205$^+$ TECs, indicating maintenance/differentiation of cTEC lineage (Figure 4F).

In summary, the prospective isolation of purified adult TEC subsets for investigating in vivo multilineage potential confirmed that the TEC^{lo} subset was enriched for TEPCs. These TEPCs could generate the major TEC lineages commonly observed within the adult thymus, including TEC^{lo}, cTEC^{hi}, mTEC^{lo}, mTEC^{hi}, and Aire$^+$ subsets within long-term reaggregate grafts.

TEPCs Form Colonies and Self-Renew within a 3D In Vitro Culture System

Clonal assays have long been used to identify stem/progenitor cells in many tissues. However, in contrast to most other epithelia, adult TECs exist as a complex 3D meshwork; 2D monolayer culture of TECs abolishes Foxn1 expression and consequently TEC function (Anderson et al., 1998). We therefore sought to overcome the current in vitro limitations by establishing a 3D coculture system that imitates in vivo TEC organization. To monitor Foxn1 expression levels, we utilized *Foxn1*$^{eGFP/+}$ knockin reporter mice that faithfully report Foxn1 expression at the transcriptional and protein level (Figures S4A and S4B). In adult *Foxn1*$^{eGFP/+}$ mice, enhanced GFP (eGFP) was expressed by the majority of TECs and represented throughout the TEC subsets (Figure S4C). TEC subsets were isolated from adult *Foxn1*$^{eGFP/+}$ mice and embedded in 50% Matrigel with supporting mouse embryonic fibroblasts in transwell inserts and cultured at the air-liquid interface in modified TEC media (Röpke, 2002).

Adult TEC subsets were cultured at increasing cell densities to evaluate colony-forming efficiency (CFE) within 3D in vitro cultures. After 1 week, colony formation was observed by a fraction of purified TEC^{lo} (CFE 0.3% ± 0.02%). The level of clonogenicity was significantly increased compared to cTEC^{hi} (0.04% ± 0.003%) and mTEC^{hi} (0.04% ± 0.005%) cultures (Figure 5A), once again supporting the presence of an enriched TEPC subset exclusively within the TEC^{lo} population. Colony formation was rare within adult mTEC^{lo} cultures (0.002% ± 0.002%) and likely requires additional factors for their survival and in vitro differentiation (Pinto et al., 2013). Clonal origin was confirmed as before using serial dilutions of mixed RFP$^+$/GFP$^+$ TEC^{lo}, where 100% formed monochromatic colonies consisting of either GFP$^+$ or RFP$^+$ TECs (Figures 5B and 5C).

The colonies were uniformly spherical, presented defined borders, and expressed both eGFP reporter fluorescence and Foxn1 protein throughout the majority of cells (Figures 5D and 5E). Immunofluorescent antibody staining revealed all colonies contained K5$^+$ K8$^+$ double-positive and K5$^-$ K8$^+$ single-positive TECs, indicating colonies of mixed TEC lineage (Figure 5E); no colonies were observed that consisted entirely of K5$^+$ or K8$^+$ cells alone. FACS analysis of dissociated colonies established from passage 1 (P1) TEC^{lo} cultures demonstrated a prominent EpCAM$^+$ eGFP$^+$ subset, of which the majority coexpressed α6-integrin (96.8% ± 0.5%) and Sca-1 (95.4% ± 2.2%; Figure 5F). Interestingly, upregulation of UEA-1 was observed in TEPC cultures, indicating entry into the mTEC lineage (Figure 5G). Importantly, repurification of EpCAM$^+$ UEA-1 negative (neg), intermediate (int), and high fractions revealed colony-forming potential was confined to the UEA-1-negative fraction (Figure 5G). No significant colony formation was observed upon passage of initial cTEC^{hi}, mTEC^{hi}, and mTEC^{lo} cultures in this system (data not shown).

Fractionation of the TEC^{lo} subset based on high, intermediate, and low levels of α6/Sca-1 surface expression (Figure 6A) revealed colony formation was enriched within the α6^{hi}Sca-1^{hi} TEPC subset (~3.5-fold) compared to whole, unfractionated TEC^{lo} (Figure 6B). Minimal enrichment was also observed within TEC^{lo} positive for the mammary SC marker, CD24 (heat stable antigen; Shackleton et al., 2006; ~1.5-fold), and the MTS24$^-$ TEC^{lo} subset (~1.6; Figures 6A and 6B).

(G) Plots show TEC subsets from adult thymus (far left plot), purified TEC^{lo} (input plot), and GFP$^+$ TECs recovered from individual TEC^{lo} reaggregate grafts at 1 (n = 3), 3 (n = 4), 6 (n = 6), and 12 (n = 3) weeks postengraftment; TEC subset gates are set according to internal WT controls at each time point; dot plots are representative.
See also Figure S3.

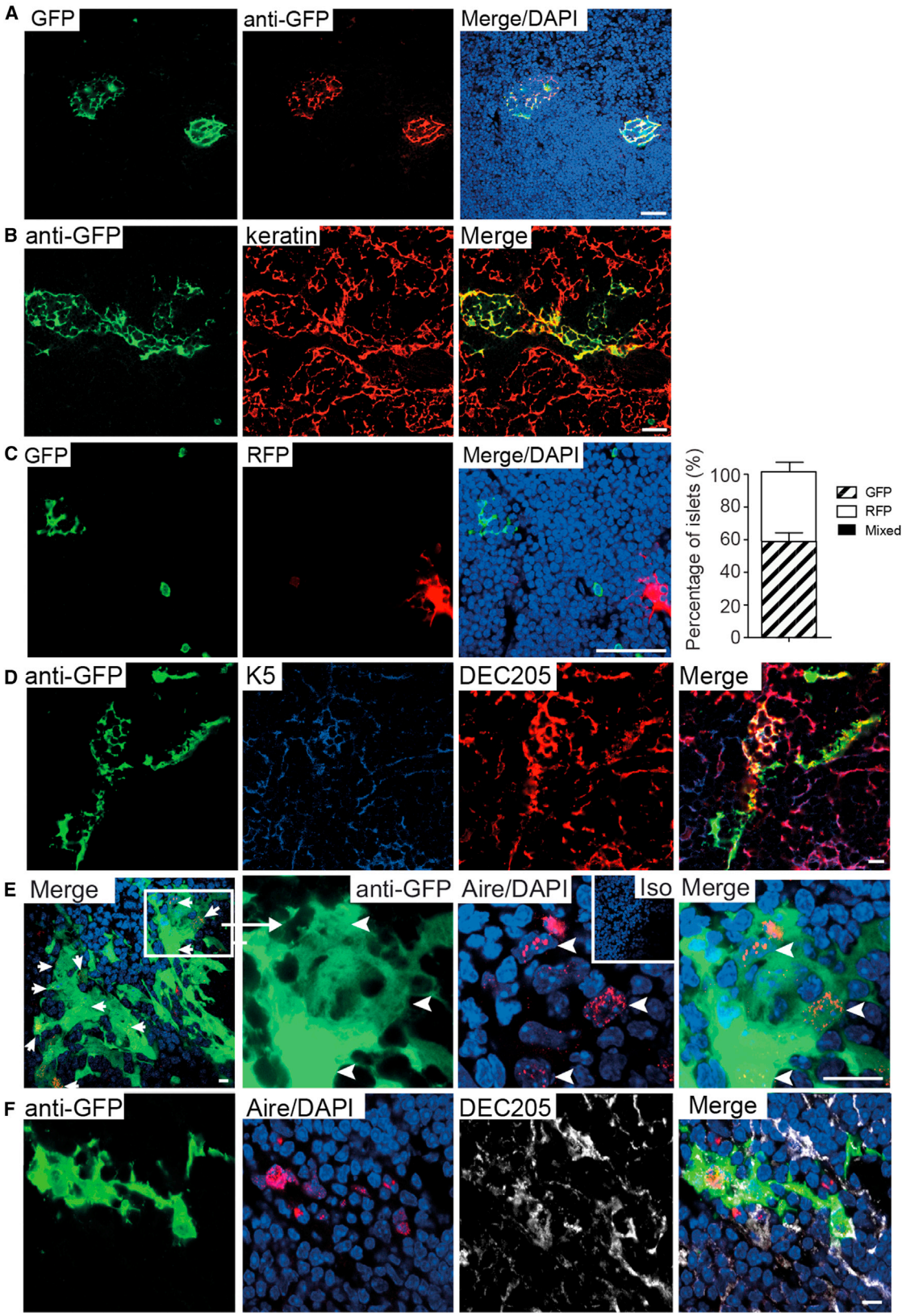

(legend on next page)

To assess the retention of thymic epithelial identity following in vitro culture, *Foxn1*$^{eGFP/+}$ TEPC-derived colonies were FACS purified at day 7, reaggregated with fetal thymic stroma, and grafted under the kidney capsule of B6 mice to allow ectopic thymus formation as previously described. At 4 weeks, immunohistological analysis of thymic grafts revealed that adult TEPCs had integrated into the thymic microenvironment, forming islets of keratin$^+$ eGFP$^+$ cells, similar to those previously observed upon reaggregation of freshly purified TEPCs (Figure 6C). Adult TECs were found to maintain Foxn1 expression (as detected by reporter GFP fluorescence), indicative of ongoing TEC function within thymic grafts (Figure 6C). Furthermore, GFP$^+$ DEC205$^+$ cTECs (Figure 6D) as well as GFP$^+$ Aire$^+$ mTECs (Figures 6E and 6F) were detected, indicating differentiation into downstream lineages. These findings suggest that adult TEPCs retained their progenitor potential following 3D in vitro culture, including the capacity to self-renew and differentiate into downstream TEC lineages when reintroduced to an in vivo thymic microenvironment.

DISCUSSION

Most epithelial tissues are maintained by a pool of multipotent stem cells and/or unipotent progenitors, which regulate cellular homeostasis and tissue repair throughout adult life (Blanpain et al., 2007). An understanding of postnatal TEC maintenance and the lineage relationship between adult TEC subsets has been limited by the lack of functional assays to support the growth/differentiation of candidate TEPCs. Our experiments, based on phenotypic dissection of adult TEC subsets, combined with in vitro culture and in vivo transplantation assays, demonstrated that significant progenitor potential in the adult thymus was retained almost exclusively within the TEC$^{lo}\alpha6^{hi}$Sca-1^{hi} subset, enriched for hallmark features of stem/progenitor function. TEPCs exhibited key properties of stem/progenitor activity, including in vivo quiescence, the capacity to self-renew, and the generation of cTEC and mTEC lineages, including the specialized Aire$^+$ subset essential for immunological tolerance. Our findings represent an example of a prospectively isolated and functionally validated TEPC from postnatal tissue.

When purified adult TEC subsets were reaggregated with fetal thymus and transplanted under the kidney capsule, TEPCs were found to be enriched within the TEC^{lo} subset and gave rise to multiple downstream subsets, including Aire$^+$ cells. Analysis of chimeric grafts at sequential time points revealed a stepwise development in which TEPCs differentiated into mTEC^{lo} via the upregulation of UEA-1, before the appearance of mTEC^{hi} cells. The temporal emergence of mTEC^{lo} prior to mTEC^{hi} in our RTOC system strongly supports the precursor-progeny relationship between these two subsets as previously reported (Gäbler et al., 2007; Gray et al., 2007; Pinto et al., 2013). Moreover, mTEC^{hi} maintenance over the 12-week in vivo culture period suggests continual replenishment, given their reported turnover of 7–10 days (Gray et al., 2006; Metzger et al., 2013). This indicates TEPCs also contain stem-cell-like capacity, demonstrating not only lineage diversity but also a degree of self-renewal in order to continually maintain downstream immature (mTEC^{lo}) and mature (mTEC^{hi}) TEC subsets within reaggregate grafts. Collectively, our data reveal that stem/progenitor potential in the postnatal thymus is localized within the TEC$^{lo}\alpha6^{hi}$Sca-1^{hi} subset and reveal a progressive developmental hierarchy in which adult TEPCs give rise to downstream mTEC^{lo} and mTEC^{hi} subsets, as well as cTEC^{hi} lineage, while maintaining a progenitor subset.

The TEPC subset likely contains additional cellular heterogeneity. The generation of downstream TEC subsets observed in this study theoretically may be the result of bipotent progenitors or a combination of multiple progenitors with restricted TEC lineage potential (Rodewald et al., 2001; Bleul et al., 2006). Previous 2D culture of fetal/adult rat TECs reported a phenotypic mix of mTEC/cTEC-restricted (unipotent) as well as mixed-lineage (bipotent) clones (Bonfanti et al., 2010). Interestingly, 100% of in vitro TEPC clones generated within this study contained a mix of K5$^+$ K8$^+$ and K5$^-$ K8$^+$ TECs, indicating heterogeneity within downstream TEC progeny and mixed lineage phenotype. In addition, clonal islets identified within in vivo reaggregate grafts routinely contained TECs that expressed the cortical marker DEC205, as well as the mTEC/cortico-medullary junction marker K5, indicating the majority of TEPCs could generate both medullary and cortical lineage. Some islets also contained Aire$^+$ TECs, representing further maturation of the mTEC lineage. Altogether, the coexpression of both cTEC (K8/DEC205) and mTEC (K5/Aire) markers within TEC clones indicates that some adult TEPCs harbor bipotent potential, as previously reported for fetal (Rossi et al., 2006) and postnatal thymus (Bleul et al., 2006). However, the low frequency of mature, GFP$^+$ Aire$^+$ TECs observed within TEPC grafts by immunohistology is noteworthy, given the substantial percentage of the mTEC^{hi} subset (containing Aire$^+$ TECs) recovered within TEPC-reaggregate grafts by flow cytometry. This disparity may be explained by the rapid turnover of Aire$^+$ mTEC^{hi} cells and transitioning into post-Aire-expressing mTEC^{lo} cells (Metzger et al., 2013). It is also possible that the adult TEPC population identified in this study is heterogeneous in regards to lineage potential and/or inefficient in the ability to generate Aire$^+$ lineage.

Although relatively quiescent in vivo, TEPCs demonstrated a significant capacity to proliferate in vitro. Whereas only a fraction (~0.3%) of the broad TEC^{lo} subset generated colonies, further

Figure 4. Adult Thymic Epithelial Progenitors Generate Clonal Islets

(A–E) Images show islets within 6-week GFP$^+$ TEPC reaggregate grafts.

(A) GFP$^+$ (green) epithelial clusters colocalize with anti-GFP (red) antibody.

(B) GFP$^+$ epithelial pockets, detected with anti-GFP (green) and antikeratin (red) staining.

(C) Isolated clusters of GFP$^+$ and RFP$^+$ TECs were detected in reaggregate grafts containing equal numbers of purified GFP$^+$/RFP$^+$ TEPCs (DAPI, blue); bar graph shows the average percentage GFP$^+$, RFP$^+$, or mixed islets (+SD) from a total of 49 islets.

(D) Expression of DEC205 and K5 within islets.

(E and F) Detection of (E) Aire$^+$ and (F) Aire$^+$/DEC205$^+$TECs within GFP$^+$ islets.

The scale bars represent (A–C) 50 μm and (D–F) 10 μm. Images are representative of n = 4–8 from two to three individual grafts.

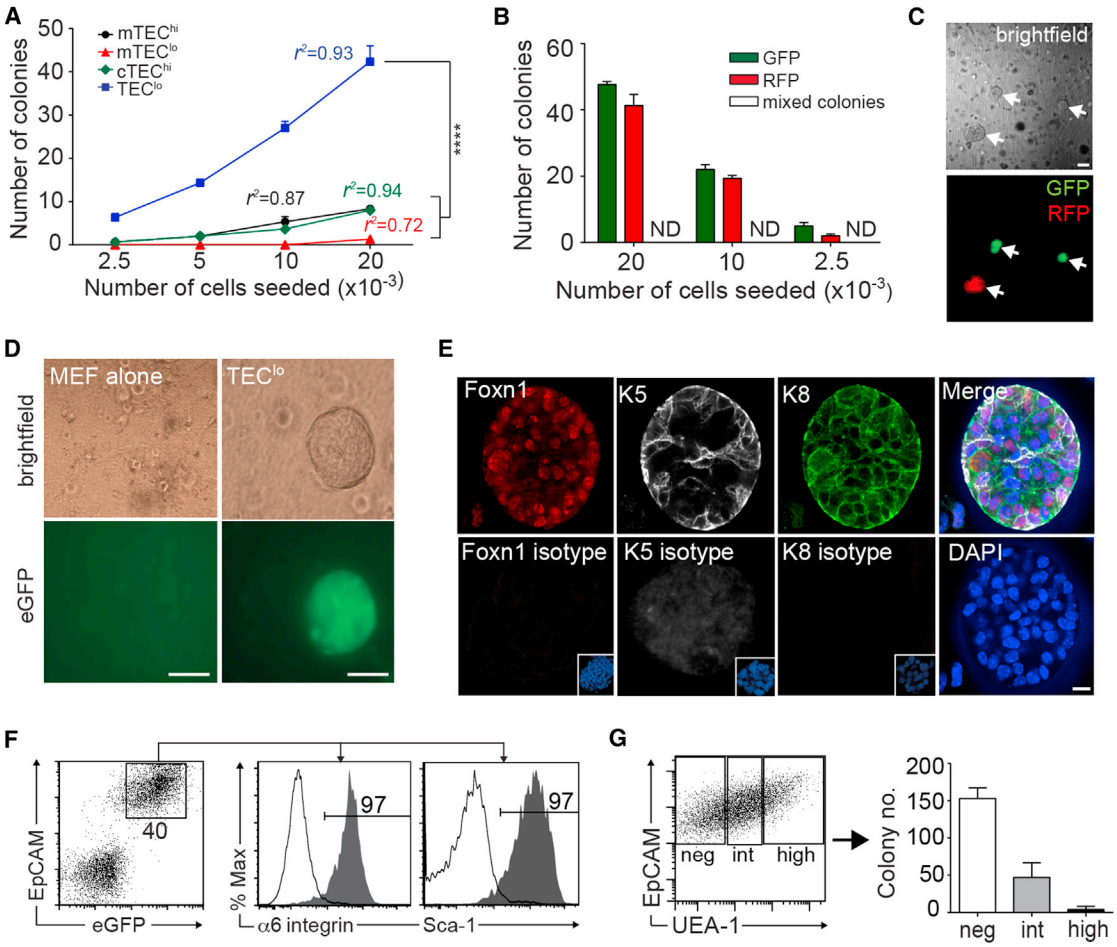

Figure 5. Adult Thymic Epithelial Progenitors Form Colonies in 3D Cultures

(A) Colony-forming efficiency of purified TEC^{lo}, cTEC^{hi}, mTEC^{lo}, and mTEC^{hi} subsets after 1 week in culture. Values represent mean colony number (+SEM; ****$p < 0.0001$) of triplicate wells with linear regression values, r^2, indicated.

(B) Bar graph shows the mean colony number (+SEM) of triplicate wells established from mixed GFP/RFP (1:1) TEC^{lo} cultures at increasing cell densities.

(C) Representative overlay image of RFP$^+$ or GFP$^+$ colonies (white arrows) derived from TEC^{lo} cultures (scale bar represents 50 μm).

(D) Representative image of cultures of the mouse embryonic fibroblast feeders alone and a colony derived from TEC^{lo} cultures at passage 1 (P1), showing eGFP (Foxn1) reporter fluorescence (scale bars represent 50 μm).

(E) P1 TEPC colonies were fixed and stained with anti-Foxn1 (red), anti-keratin 8 (K8, green), and anti-keratin 5 (K5, gray) with DAPI (blue); representative of $n > 20$ (scale bar represents 10 μm).

(F) Flow cytometric analysis of P1 TEPC cultures demonstrates a prominent EpCAM$^+$ eGFP$^+$ subset, which expresses α6 integrin and Sca-1 (isotype control, black line).

(G) EpCAM$^+$ eGFP$^+$ TECs from P1 TEPC cultures express negative (neg), intermediate (int), and high levels of UEA-1. Resorting indicates colony-forming potential was enriched within the UEA-1 neg subset (mean colony number +SD). Dot plots ($n = 3–5$) and images ($n > 10$) are representative. All data are representative of two to three independent experiments.

See also Figure S4.

purification of TEPCs based on high-level α6/Sca-1 expression, and to a lesser extent, positive expression of CD24 and negative expression of MTS24, resulted in enhanced colony frequency. Whereas survival of TEPCs within the current in vitro system may be limited, when returned to an in vivo fetal thymic microenvironment, in vitro cultured TEPCs reformed islets, including the generation and maintenance of Foxn1$^+$ cTEC, mTEC, and Aire$^+$ lineage over a period of weeks. The persistence of adult TEPCs over serial transfer between in vitro and in vivo culture systems indicates they harbor a capacity to self-renew and retain thymic identity in culture.

In this study, we identify and characterize the stem/progenitor function of an adult TEPC subset and reveal phenotypic differences between fetal and adult progenitors, including the upregulation of Sca-1 and high-level α6 integrin expression following birth. Whereas resident LRCs and in vitro colony-forming progenitors were preferentially enriched within TEPCs of α6^{hi}Sca-1^{hi} phenotype, reaggregate thymic grafts revealed the capacity

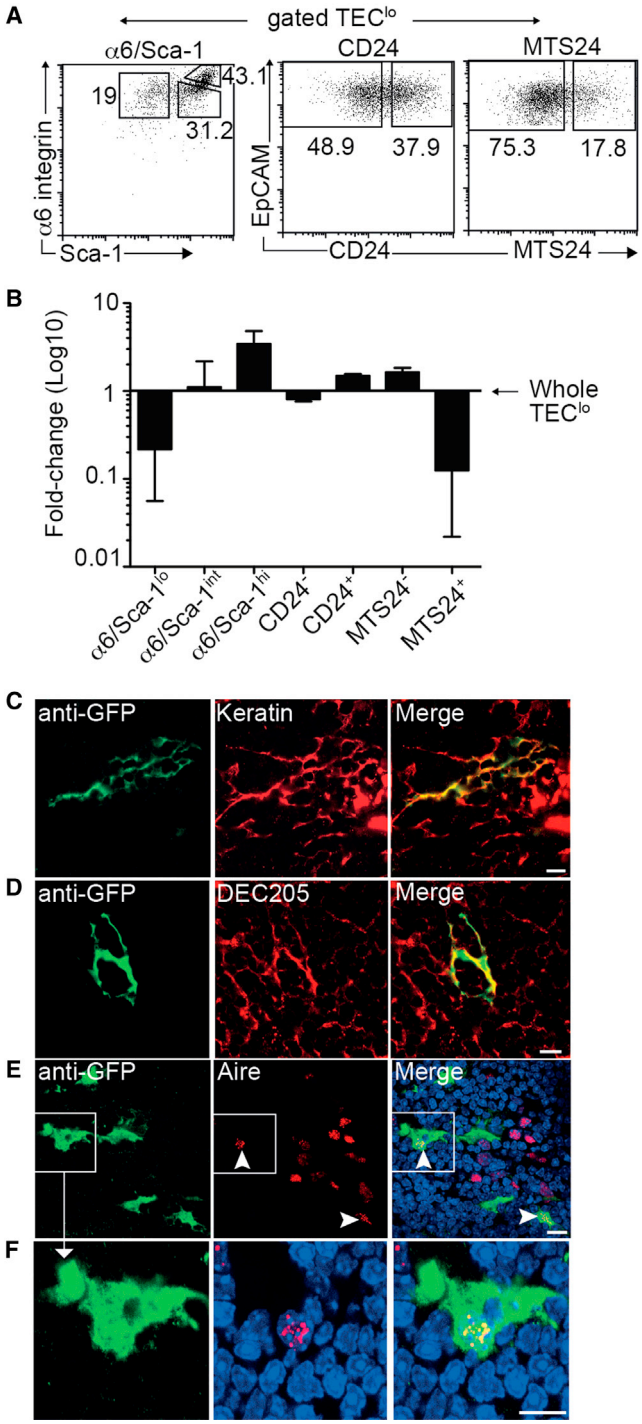

Figure 6. Enriched Colony Formation and Generation of TEC Lineage within In Vivo Grafts

(A) Plots show the expression of stem cell markers within phenotypically defined TEC^{lo} (gated CD45$^-$ EpCAM$^+$ MHCII^{lo} UEA-1$^-$).

(B) TEC^{lo} subsets defined in (A) were FACS purified and assessed within 3D cultures for colony formation. Graph shows fold change of percentage colony-forming efficiency within individual subsets, normalized against the unsorted TEC^{lo} fraction (value = 1).

(C–F) P1-cultured TEPCs were purified, reaggregated with fetal thymus, and ectopically engrafted. Histology of 4-week grafts show presence of GFP$^+$ adult TECs and colocalization with TEC lineage markers, keratin (C); cortical TEC marker, DEC205 (D); and the mature mTEC lineage marker, Aire (E and F). (F) shows the inset in (E). All images are representative (n = 2). The scale bars represent 10 μm.

to differentiate into downstream TEC lineages was still maintained when α6 integrin expression was slightly downregulated (α6^{int}Sca-1^{hi}). Combined, these data suggest that enhanced properties of self-renewal within the adult TEPC pool may be phenotypically reflected by gradient increases in α6/Sca-1 expression levels, similar to that reported in other epithelial compartments.

Thus, high level of integrin expression observed on the adult TEPC subset may function in situ to preferentially bind cells within a defined stromal niche, where they would be subject to extrinsic regulation of cell division and/or differentiation in steady-state tissue (Chen et al., 2013). The localization of LRCs to the cortico-medullary junction (CMJ) suggests this region may regulate progenitor function in the adult thymus, where TEPCs are ideally situated to generate compartment-specific progenitors of the mTEC and cTEC lineages (Alves et al., 2009; Lee et al., 2011). Subsequently, the downregulation of integrins in response to activating stimuli may initiate the migration of progenitors away from the SC niche to a pathway of amplification and differentiation. Dissection of the molecular controls that govern TEPC maintenance within the putative CMJ niche will be critical for any effort to harness their potential.

In summary, our studies demonstrate an example of significant progenitor potency within a defined TEC subset isolated from adult tissue. The identification of an adult TEPC subset provides a focal point for developing an understanding of their molecular regulation, homeostasis and differentiation, and role in thymic degeneration with age, potentially enabling a more directed approach to inducing TEC regeneration.

EXPERIMENTAL PROCEDURES

Animals

Adult C57BL6/J (B6) mice, B6 transgenic eGFP mice (eGFP expression driven by the chicken β-actin promoter), and B6 transgenic RFP mice (RFP expression driven by pβactin-CMV-DsRed T3 transgene) were used. The generation of the *Foxn1*$^{eGFP/+}$ knockin mouse line is described in the Supplemental Experimental Procedures S1. B6 mice aged 6 to 7 weeks were used as graft recipients. Embryonic thymuses were obtained from day 14.5 embryos (E14.5), where the presence of a vaginal plug was designated as E0.5. All animals were bred and housed at Monash University Central Animal Services (Monash University) according to ethical and institutional guidelines. All adult mice used in this study were aged between 6 and 8 weeks unless otherwise stated.

BrdU Pulse and Chase

Adult B6 mice were injected intraperitoneally with 1 mg of BrdU (Sigma-Aldrich) in PBS. Animals were maintained on 0.5 mg/ml BrdU in drinking water with 3.3 mg/ml artificial sweetener (Equal) for a total of 12 days (pulse) before replacement with normal water for the chase period of 1–6 months. Control mice were injected with PBS and maintained on normal drinking water.

Individual and Pooled Thymus Digestion

Individual thymus or pools of 10–20 thymuses were digested as previously described (Seach et al., 2012) in RPMI-1640 containing 1U/ml Liberase TM supplemented with 0.02% (w/v) DNase I (all enzymes from Roche). For analysis of DEC205 expression, thymus digestion was performed in 0.125% (w/v) collagenase/DNase due to epitope cleavage during Liberase digestion. Individual

thymic digests were stained immediately with antibodies for FACS analysis. To remove thymocytes before TEC isolation, pooled thymic digests were incubated with CD45 MicroBeads (Miltenyi Biotec) and depleted using the AutoMACS machine (Miltenyi Biotec) as previously described (Seach et al., 2012).

Flow Cytometric Analysis

We stained 5 × 10^6 cells from individual thymic digests with surface markers as indicated. One hundred nanograms per milliliter propidium iodide (Sigma-Aldrich) was used to exclude dead cells. For intracellular β5t staining, following surface staining, cells were fixed and permeabilized in BD Cytofix/Cytoperm buffer (BD Biosciences) and incubated with anti-β5t for 20 min, followed by secondary antibody incubation. Intracellular staining for BrdU was performed as previously described (Gray et al., 2007). Cells were acquired using a BD FACSCanto II flow cytometer (BD Biosciences). All FACS data were analyzed using FlowLogic software v400.1A (Inivai Technologies).

Thymic Epithelial Cell Separation

TECs were prestained with CD45, MHCII, EpCAM, UEA-1, and Ly51 immunoconjugates with the addition of α6-integrin, Sca-1, MTS24, and CD24 antibodies where indicated. Sorting was performed using a BD Influx I cell sorter (BD Biosciences) using a 100 μM nozzle at 20 psi and at 3,000 events per second. Adult TEC subsets were counted and used directly in functional RTOC/3D culture assays or snap frozen in liquid nitrogen for RNA extraction.

RTOC

RTOCs were performed as recently described (Seach et al., 2013). Briefly, E14.5 thymic lobes were enzymatically digested and reaggregated with GFP^+ adult TEC subsets at a ratio of 5:1. Typically, between 7.5 × 10^4 and 1 × 10^5 adult TECs were added per RTOC. Reaggregates were incubated overnight (18 hr) at 37°C (5% CO_2) before engraftment under the kidney capsule of B6 adult male recipients. Grafts were harvested between 1 and 12 weeks and enzymatically digested for FACS analysis or snap frozen for immunofluorescence (IF).

3D Thymic Epithelial Cultures

3D TEC cultures were based on a recent protocol (McQualter et al., 2010). Specifically, *Foxn1*$^{eGFP/+}$ TEC subsets were FACS purified and combined with 2 × 10^5 irradiated mouse embryonic fibroblasts. Cells were resuspended in 50% Matrigel (catalog number 356231; BD Biosciences), plated into 24-well 0.4 μM transwell inserts (Millipore), and allowed to set for 10 min at 37°C before adding TEC media (Röpke, 2002; RPMI-1640 with 10% fetal bovine serum, 55 μM 2-mercaptoethanol, 10 mM HEPES, 1 × 10^3 U/ml penicillin, 1 × 10^4 μg streptomycin, 2 mM GlutaMAX, 1 mM sodium pyruvate, 0.1 mM nonessential amino acids, 5 μg/ml insulin, 2.75 μg/ml transferrin, 3.35 ng/ml selenium, 2 × 10^{-9} M 3,3′,5-triiodo-L-thyronine, 0.4 μg/ml hydrocortisone, 24 μg/ml adenine, 1 × 10^{-10} M cholera toxin, 0.0002% [v/v] heparin, and 20 ng/ml keratinocyte growth factor [R&D Systems]). Cultures were incubated under low oxygen conditions (5% O_2, 10% CO_2, and 85% N_2). To digest colonies, transwell inserts were washed with PBS and digested with 0.25% (v/v) trypsin/EDTA (Life Technologies) and filtered through a 100 μM nylon mesh.

RTOCs of 3D Cultured TECs

Colonies established from primary TEC^{lo} 3D cultures (1 week; P1) were enzymatically digested and FACS purified ($EpCAM^+$). Sorted TECs (between 2 × 10^4 and 1 × 10^5) were reaggregated with whole E14.5 thymic cells (5 × 10^5) and engrafted under the kidney capsule as per RTOC protocol. Grafts were harvested after 4 weeks and prepared for IF analysis described below.

Immunofluorescence Analysis

Preparation and immunofluorescent staining of thymic lobes, kidney/thymic grafts, and transwell inserts is described in the Supplemental Experimental Procedures S2.

qPCR

An outline of the quantitative PCR (qPCR) procedure is described in the Supplemental Experimental Procedures S3.

Statistical Analysis

All values are expressed as the mean ± SEM, unless otherwise specified. Statistical analysis was performed using the nonparametric Mann-Whitney U test (two-tailed) and unpaired t test using GraphPad Prism v6.02 software (GraphPad Software). A p value $\leq$ 0.05 was considered statistically significant.

SUPPLEMENTAL INFORMATION

Supplemental information includes Supplemental Experimental Procedures and four figures and can be found with this article online at http://dx.doi.org/10.1016/j.celrep.2014.07.029.

AUTHOR CONTRIBUTIONS

A.P.C., R.L.B., and N.L.L. contributed the conceptual design. A.P.C., N.L.L., and K.W. contributed the main experimental design with intellectual input from R.L.B. and D.H.G. Experiments were performed by K.W. and N.L.L with assistance from M.B., J.M.C.L., M.V.H., D.M.K., and C.S. The manuscript was written and prepared by N.L.L., K.W., and A.P.C. with editorial assistance from R.L.B. and D.H.G.

ACKNOWLEDGMENTS

The authors would like to acknowledge Jade Homann for her expert mouse surgery and Dr. Jonathan McQualter and Professor Ivan Bertoncello for their technical assistance with the 3D transwell assays; A/Prof Sharon Ricardo (Renal Regeneration Group, Monash University) and Dr. Susie Nilsson at Commonwealth Scientific and Industrial Research Organization (CSIRO) for providing GFP and RFP mice, respectively; Dr. Judy Callaghan and the team at Monash Micro Imaging (Monash University) for their scientific and technical assistance; and the team at Flowcore (Monash University) for their expert cell sorting. This work was supported by grants from the Australian Stem Cell Centre, the Victoria-California Stem Cell Alliance (DIIRD/CIRM), and the National Health and Medical Research Council of Australia (NH&MRC).

Received: February 7, 2014
Revised: May 4, 2014
Accepted: July 17, 2014
Published: August 14, 2014

REFERENCES

Adams, J.M., and Cory, S. (1998). The Bcl-2 protein family: arbiters of cell survival. Science *281*, 1322–1326.

Alves, N.L., Richard-Le Goff, O., Huntington, N.D., Sousa, A.P., Ribeiro, V.S., Bordack, A., Vives, F.L., Peduto, L., Chidgey, A., Cumano, A., et al. (2009). Characterization of the thymic IL-7 niche in vivo. Proc. Natl. Acad. Sci. USA *106*, 1512–1517.

Anderson, G., and Jenkinson, E.J. (2001). Lymphostromal interactions in thymic development and function. Nat. Rev. Immunol. *1*, 31–40.

Anderson, G., and Takahama, Y. (2012). Thymic epithelial cells: working class heroes for T cell development and repertoire selection. Trends Immunol. *33*, 256–263.

Anderson, K.L., Moore, N.C., McLoughlin, D.E., Jenkinson, E.J., and Owen, J.J. (1998). Studies on thymic epithelial cells in vitro. Dev. Comp. Immunol. *22*, 367–377.

Baik, S., Jenkinson, E.J., Lane, P.J., Anderson, G., and Jenkinson, W.E. (2013). Generation of both cortical and Aire(+) medullary thymic epithelial compartments from CD205(+) progenitors. Eur. J. Immunol. *43*, 589–594.

Bennett, A.R., Farley, A., Blair, N.F., Gordon, J., Sharp, L., and Blackburn, C.C. (2002). Identification and characterization of thymic epithelial progenitor cells. Immunity *16*, 803–814.

Blanpain, C., and Fuchs, E. (2006). Epidermal stem cells of the skin. Annu. Rev. Cell Dev. Biol. *22*, 339–373.

Blanpain, C., Horsley, V., and Fuchs, E. (2007). Epithelial stem cells: turning over new leaves. Cell *128*, 445–458.

Bleul, C.C., Corbeaux, T., Reuter, A., Fisch, P., Mönting, J.S., and Boehm, T. (2006). Formation of a functional thymus initiated by a postnatal epithelial progenitor cell. Nature *441*, 992–996.

Bonfanti, P., Claudinot, S., Amici, A.W., Farley, A., Blackburn, C.C., and Barrandon, Y. (2010). Microenvironmental reprogramming of thymic epithelial cells to skin multipotent stem cells. Nature *466*, 978–982.

Chen, S., Lewallen, M., and Xie, T. (2013). Adhesion in the stem cell niche: biological roles and regulation. Development *140*, 255–265.

Cheng, L., Guo, J., Sun, L., Fu, J., Barnes, P.F., Metzger, D., Chambon, P., Oshima, R.G., Amagai, T., and Su, D.M. (2010). Postnatal tissue-specific disruption of transcription factor FoxN1 triggers acute thymic atrophy. J. Biol. Chem. *285*, 5836–5847.

Chidgey, A., Dudakov, J., Seach, N., and Boyd, R. (2007). Impact of niche aging on thymic regeneration and immune reconstitution. Semin. Immunol. *19*, 331–340.

Chidgey, A.P., Seach, N., Dudakov, J., Hammett, M.V., and Boyd, R.L. (2008). Strategies for reconstituting and boosting T cell-based immunity following haematopoietic stem cell transplantation: pre-clinical and clinical approaches. Semin. Immunopathol. *30*, 457–477.

Depreter, M.G., Blair, N.F., Gaskell, T.L., Nowell, C.S., Davern, K., Pagliocca, A., Stenhouse, F.H., Farley, A.M., Fraser, A., Vrana, J., et al. (2008). Identification of Plet-1 as a specific marker of early thymic epithelial progenitor cells. Proc. Natl. Acad. Sci. USA *105*, 961–966.

Fuchs, E. (1990). Epidermal differentiation. Curr. Opin. Cell Biol. *2*, 1028–1035.

Gäbler, J., Arnold, J., and Kyewski, B. (2007). Promiscuous gene expression and the developmental dynamics of medullary thymic epithelial cells. Eur. J. Immunol. *37*, 3363–3372.

Gill, J., Malin, M., Holländer, G.A., and Boyd, R. (2002). Generation of a complete thymic microenvironment by MTS24(+) thymic epithelial cells. Nat. Immunol. *3*, 635–642.

Gray, D.H.D., Seach, N., Ueno, T., Milton, M.K., Liston, A., Lew, A.M., Goodnow, C.C., and Boyd, R.L. (2006). Developmental kinetics, turnover, and stimulatory capacity of thymic epithelial cells. Blood *108*, 3777–3785.

Gray, D., Abramson, J., Benoist, C., and Mathis, D. (2007). Proliferative arrest and rapid turnover of thymic epithelial cells expressing Aire. J. Exp. Med. *204*, 2521–2528.

Hamazaki, Y., Fujita, H., Kobayashi, T., Choi, Y., Scott, H.S., Matsumoto, M., and Minato, N. (2007). Medullary thymic epithelial cells expressing Aire represent a unique lineage derived from cells expressing claudin. Nat. Immunol. *8*, 304–311.

Hayashi, R., Yamato, M., Saito, T., Oshima, T., Okano, T., Tano, Y., and Nishida, K. (2008). Enrichment of corneal epithelial stem/progenitor cells using cell surface markers, integrin alpha6 and CD71. Biochem. Biophys. Res. Commun. *367*, 256–263.

Haynes, B.F., Markert, M.L., Sempowski, G.D., Patel, D.D., and Hale, L.P. (2000). The role of the thymus in immune reconstitution in aging, bone marrow transplantation, and HIV-1 infection. Annu. Rev. Immunol. *18*, 529–560.

Hiyama, E., and Hiyama, K. (2007). Telomere and telomerase in stem cells. Br. J. Cancer *96*, 1020–1024.

Jenkinson, E.J., Anderson, G., and Owen, J.J. (1992). Studies on T cell maturation on defined thymic stromal cell populations in vitro. J. Exp. Med. *176*, 845–853.

Jenkinson, W.E., Rossi, S.W., Parnell, S.M., Jenkinson, E.J., and Anderson, G. (2007). PDGFRalpha-expressing mesenchyme regulates thymus growth and the availability of intrathymic niches. Blood *109*, 954–960.

Lee, E.N., Park, J.K., Lee, J.R., Oh, S.O., Baek, S.Y., Kim, B.S., and Yoon, S. (2011). Characterization of the expression of cytokeratins 5, 8, and 14 in mouse thymic epithelial cells during thymus regeneration following acute thymic involution. Anat Cell Biol *44*, 14–24.

McQualter, J.L., Yuen, K., Williams, B., and Bertoncello, I. (2010). Evidence of an epithelial stem/progenitor cell hierarchy in the adult mouse lung. Proc. Natl. Acad. Sci. USA *107*, 1414–1419.

Metzger, T.C., and Anderson, M.S. (2011). Control of central and peripheral tolerance by Aire. Immunol. Rev. *241*, 89–103.

Metzger, T.C., Khan, I.S., Gardner, J.M., Mouchess, M.L., Johannes, K.P., Krawisz, A.K., Skrzypczynska, K.M., and Anderson, M.S. (2013). Lineage tracing and cell ablation identify a post-Aire-expressing thymic epithelial cell population. Cell Rep *5*, 166–179.

Morris, R.J., Liu, Y., Marles, L., Yang, Z., Trempus, C., Li, S., Lin, J.S., Sawicki, J.A., and Cotsarelis, G. (2004). Capturing and profiling adult hair follicle stem cells. Nat. Biotechnol. *22*, 411–417.

Ohigashi, I., Zuklys, S., Sakata, M., Mayer, C.E., Zhanybekova, S., Murata, S., Tanaka, K., Holländer, G.A., and Takahama, Y. (2013). Aire-expressing thymic medullary epithelial cells originate from β5t-expressing progenitor cells. Proc. Natl. Acad. Sci. USA *110*, 9885–9890.

Pinto, S., Schmidt, K., Egle, S., Stark, H.J., Boukamp, P., and Kyewski, B. (2013). An organotypic coculture model supporting proliferation and differentiation of medullary thymic epithelial cells and promiscuous gene expression. J. Immunol. *190*, 1085–1093.

Rode, I., and Boehm, T. (2012). Regenerative capacity of adult cortical thymic epithelial cells. Proc. Natl. Acad. Sci. USA *109*, 3463–3468.

Rodewald, H.R., Paul, S., Haller, C., Bluethmann, H., and Blum, C. (2001). Thymus medulla consisting of epithelial islets each derived from a single progenitor. Nature *414*, 763–768.

Röpke, C. (2002). Thymic epithelial cell culture. Methods Mol. Biol. *188*, 27–36.

Rossi, S.W., Jenkinson, W.E., Anderson, G., and Jenkinson, E.J. (2006). Clonal analysis reveals a common progenitor for thymic cortical and medullary epithelium. Nature *441*, 988–991.

Seach, N., Wong, K., Hammett, M., Boyd, R.L., and Chidgey, A.P. (2012). Purified enzymes improve isolation and characterization of the adult thymic epithelium. J. Immunol. Methods *385*, 23–34.

Seach, N., Hammett, M., and Chidgey, A. (2013). Isolation, characterization, and reaggregate culture of thymic epithelial cells. Methods Mol. Biol. *945*, 251–272.

Senoo, M., Pinto, F., Crum, C.P., and McKeon, F. (2007). p63 Is essential for the proliferative potential of stem cells in stratified epithelia. Cell *129*, 523–536.

Shackleton, M., Vaillant, F., Simpson, K.J., Stingl, J., Smyth, G.K., Asselin-Labat, M.L., Wu, L., Lindeman, G.J., and Visvader, J.E. (2006). Generation of a functional mammary gland from a single stem cell. Nature *439*, 84–88.

Shakib, S., Desanti, G.E., Jenkinson, W.E., Parnell, S.M., Jenkinson, E.J., and Anderson, G. (2009). Checkpoints in the development of thymic cortical epithelial cells. J. Immunol. *182*, 130–137.

Terunuma, A., Kapoor, V., Yee, C., Telford, W.G., Udey, M.C., and Vogel, J.C. (2007). Stem cell activity of human side population and alpha6 integrin-bright keratinocytes defined by a quantitative in vivo assay. Stem Cells *25*, 664–669.

Tumbar, T., Guasch, G., Greco, V., Blanpain, C., Lowry, W.E., Rendl, M., and Fuchs, E. (2004). Defining the epithelial stem cell niche in skin. Science *303*, 359–363.

Wallin, J., Eibel, H., Neubüser, A., Wilting, J., Koseki, H., and Balling, R. (1996). Pax1 is expressed during development of the thymus epithelium and is required for normal T-cell maturation. Development *122*, 23–30.

Welm, B.E., Tepera, S.B., Venezia, T., Graubert, T.A., Rosen, J.M., and Goodell, M.A. (2002). Sca-1(pos) cells in the mouse mammary gland represent an enriched progenitor cell population. Dev. Biol. *245*, 42–56.

Yano, M., Kuroda, N., Han, H., Meguro-Horike, M., Nishikawa, Y., Kiyonari, H., Maemura, K., Yanagawa, Y., Obata, K., Takahashi, S., et al. (2008). Aire controls the differentiation program of thymic epithelial cells in the medulla for the establishment of self-tolerance. J. Exp. Med. *205*, 2827–2838.